American Journal of Botany and Bioengineering
https://biojournals.us/index.php/AJBP
ISSN: 2997-9331

Preparation of Nanomaterial Thin Film as Saturable Absorber

Tabarak sadiq Tuman Aliwi
Technological University College of Engineering Department of Laser and Optoelectronic Engineering

Noor Alaa Jabir Tarad
University of Technology College of engineering Laser and optoelectronics engineering department

Elaf abdul muttalib hafez
University of Technology College of Engineering Department of Laser and Optoelectronics Engineering

Fatima Bashar Abboud Qasim
Technological University College of Engineering Department of Laser and Optoelectronics Engineering

Tabark Abbas Awad Hadi
University of Technology College of engineering Laser and optoelectronics engineering department

Jumana rafeek jafer abd alhassan
University of Technology College of engineering Laser and optoelectronics

Mariem Amer Namaa Abed Alrasool
Al-Nahrain University College of Engineering Laser and Optoelectronics Engineering Department

Received: 2024 26, Dec
Accepted: 2025 27, Jan
Published: 2025 28, Feb

Copyright © 2025 by author(s) and BioScience Academic Publishing. This work is licensed under the Creative Commons Attribution International License (CC BY 4.0).

Open Access

Abstract: In this project, an Erbium doped fiber laser (EDFL) with passive Q-switching was created employing saturable absorber (SA) composed of Zirconium Dioxide-8Ytria nanomaterial. The fabrication of SA involved the drop-casting method, with polyvinyl alcohol (PVA). SA materials were characterized using different techniques to determine their Optical and physical spectroscopic analyses. Their crystalline structure was examined using X-ray diffraction (XRD) analysis, the morphological arrangement was measured by Scanning Electron

http://creativecommons.org/licenses/by/4.0/

Microscope (SEM), and the optical characteristics were found using UV- Vis Spectrophotometer. By integrating the proposed SAs in the all-fiber ring cavity, Q-switched pulse operation generated directly using an EDF as an active medium. a stable Q-switched regime with the maximal pulse repetition rate of 52.5 kHz, the shortest pulse width of 10.5 µs, and maximum average output power up to 151.7 µW were attained at a maximum available pump power of 280 mW.

Key words: Nanomaterial Thin Film, Saturable Absorber, Zirconium Dioxide-8Ytria, Passive Q-switching, Erbium Doped Fiber Laser, Drop-casting Method, Optical Characterization.

Chapter One Introduction

1. Introduction

Pulsed fiber lasers find many uses ranging from fiber sensors such as range finders and gas or pressure sensors [1], optical time-domain reflectometry (OTDR) where high-power ultrafast laser pulses are required for accuracy in measurements [2], and numerous nonlinear optical purposes like harmonic generation or pumping of an acousto-optically gain-switched solid state crystal laser [3]. The all-fiber construction has some advantages compared to other solid state pulsed lasers. For example, all-fiber construction provides inherent robustness and relative compactness. Also, keeping the light constrained to a waveguide with no open-air propagation or alignment considerations improves both the short and long term stability of the system while simultaneously eliminating many potential noise sources.

These benefits allow high pulse energy and repetition rate while maintaining ultrashort temporal durations ranging from microseconds (µs) to femtoseconds (fs). The combination of high pulse energy with ultrashort duration results in large peak powers, leading to uses in materials processing and the medical industry [4]. The incorporation of carbon nanotubes in the saturable absorbing device has advantages of its own compared to the common alternatives for creating saturable absorbers (SAs).

In large part, the SAs used for pulsed operation of fiber lasers are semiconducting saturable absorber mirrors (SESAMs), and they come with a high price tag and complex fabrication process. Additionally, the interaction of the laser light with the SESAM is limited to reflection only. Carbon nanotubes are well tailored for use as a nonlinear optical absorption material owing to their rapid saturation recovery time of ~1 picosecond (ps) or less, substantial optical damage threshold, and long-term physical and chemical reliability. There is a wide range of fabrication options for carbon nanotube (CNT) based SAs that are mostly cheaper, faster, and experimentally less complex than that of SESAMs; furthermore, the various methods of incorporating these devices into the fiber laser cavity allows for various CNT-light interaction schemes, which in turn increases laser cavity design flexibility [5].

2. Laser principle

Generation of laser radiation involves a few process that are absorption, spontaneous emission and stimulated emission. For the absorption, an electron at ground energy level (E1) absorbed an incident photon and excited to higher energy level (E2). When an electron at higher energy level (E2), in general, the electron will eventually decay to the ground energy level (E1), thus release a photon of radiation. This phenomenon is Spontaneous emission that emit photon in random direction and phase.

To generate laser, population inversion process is required. Population inversion occurs when the population at level 2 or density of excited two-level atomic system is more than population level 1 or density of the unexcited two-level atomic system ($N_2 > N1$) [6].

In this condition, the energy of E21, will enable an electron at higher energy level (E2) to decay toward ground energy level (E1). The energy can be calculated by:

hv = E21 = E2 – E1 (Eq. 1.1)

The energy of E21 will be transferred in the form of electromagnetic wave which adds to the incident photon. This event is called as stimulated emission. This stimulated emission will exhibit emission that is identical to the incident photon (same wavelength, direction and phase). But if the condition is $N_2 < N1$, the active medium acts as an absorber. Figure 1.1 shows three mechanism.

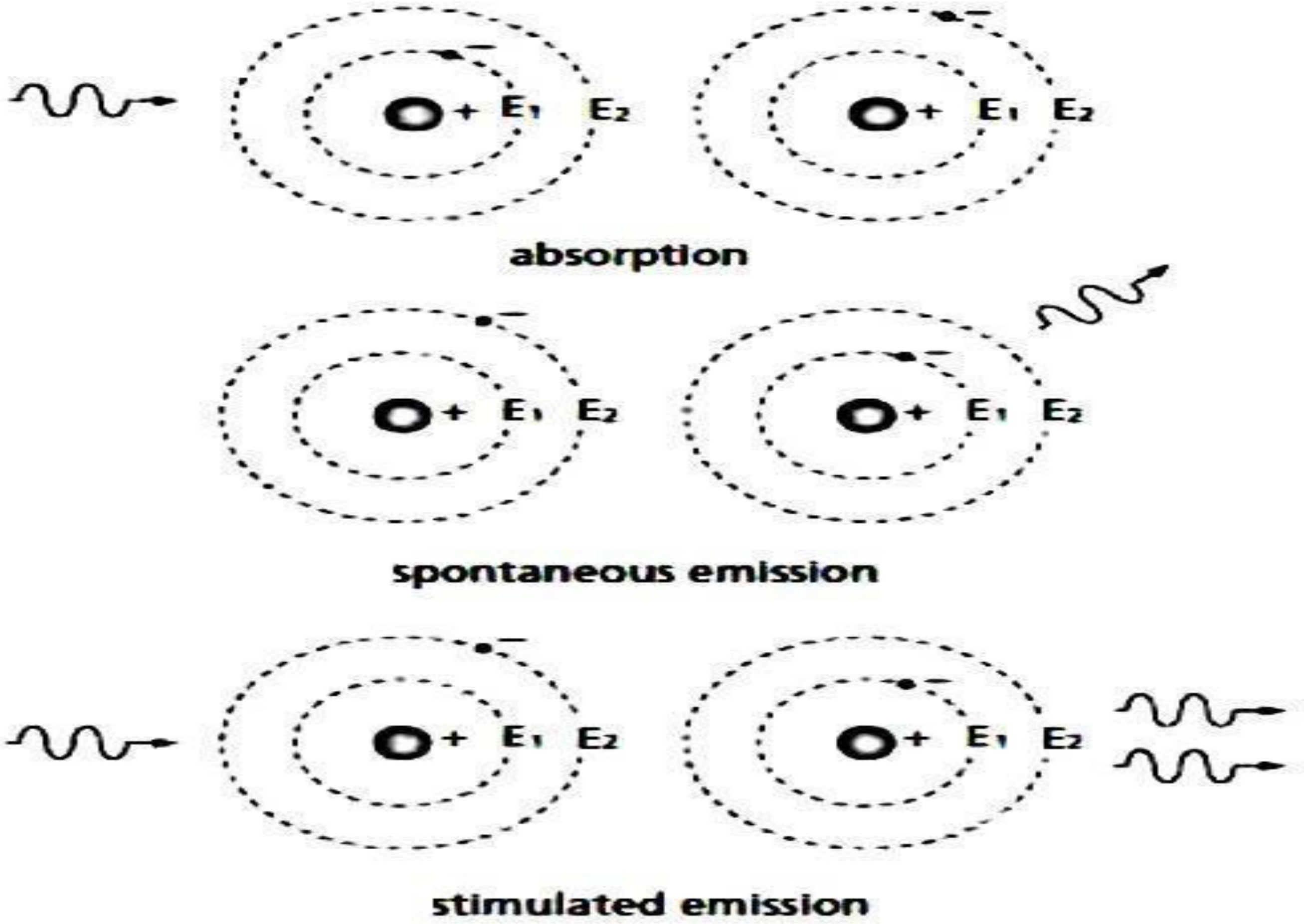

(Figure 1.1): The mechanism of absorption, spontaneous emission and stimulated emission.

3. Fiber optic

Fiber optics is light transmission over a very fine glass or plastic fibers. Light travels in fiber optics by total internal refraction principle. The remarkable discovery in optical communication by Charles K. Kao and George A. Hockham from Standard Telecommunication Laboratories, U.K came in 1966 [7]. Before their pioneering work, fiber glass was believed to have the potential to carry light. However, it was not suitable because of their excessively high loss of signal from Rayleigh scattering. In 1965, Kao and Hockham came out with theories for the fundamental limitation for glass. Using their finding, light attenuation was successfully reduced to 20dB/km.

previously, light attenuation in fiber optics was 1000dB/km. Upon after a few further investigations on the glass material, they had identified that the main problem lied in the impurities inside the material itself. Therefore, a new low-loss material was needed to tackle the problem. They experimented with various kinds of material and had identified fused- silica (SiO2) as an excellent candidate.

Their remarkable discovery triggered a rapid development in various photonics application based on fiber optics. Their discovery eventually led to winning the Nobel Prize in Physics in 2009. Due to the increase in demand for data transmission, fiber optics has become the new alternative to replace the existing copper cables.

The advantages of fiber optic compare to copper cables are:

1. Fiber optics has high signal bandwidth (200 and 600 MHz-km, for Multimode (MM) fibers and more than 10GHz for single mode (SM) fibers), while for an electrical conductor, usually is between 10 to 25MHz-km.
2. Low attenuation of fiber optics enable longer cables runs and fewer repeater.
3. Optical fibers are unaffected from any electromagnetic radiation and do not emit any radiation.
4. Optical fibers are easy to install, and their weight is 10-15 times lesser and the cost less than other.

Optical fiber construction consists of core, cladding, buffer and jacket. A small core is the medium used to transmit light and has a core/cladding diameters of 8/125 µm. To realize total internal reflection, the refraction index of the cladding is less than the index of refraction of the core. The buffer (Ø = 250 µm) and jacket (Ø = 400µm) are to protect the core and cladding from any physical and environment damage. A schematic of an optical fiber is presented in Figure 1.2.

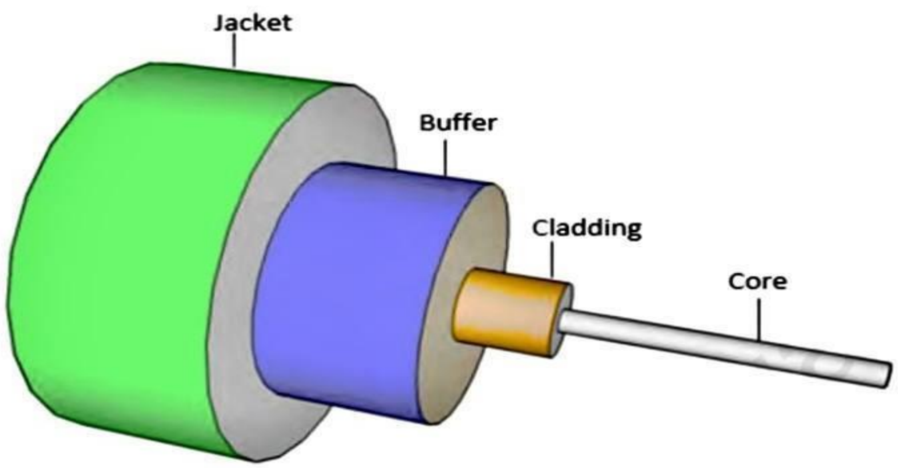

***(Figure 1.2)*: Illustrative diagram of an optical fiber.**

4. Erbium-Doped Fiber (EDF)

Since the discovery of Erbium-Doped Fiber (EDF) in late 1980s, EDF has proven to be a material which is used in various applications such as broadband optical source, wide- band optical amplifier and tunable laser. The generation of Amplified Spontaneous Emission (ASE) in EDF produces high output power and broader optical bandwidth [8]. Since demonstration of Erbium-Doped Fiber Amplifier (EDFA) as optical amplifier, they attracted much interest in optical communication industry. In fiber laser application, the Erbium-Doped Fiber Laser (EDFL) is one of a most famous gain medium.

The core of an EDF gain medium is doped with rare earth element erbium ion (Er^{3+}). The EDF became a popular gain medium in fiber laser because their large gain bandwidth, typically ranging in tens of nanometer. The energy level diagram of Er^{3+} ions is represent in Figure 1.3. The laser

974nm is pump through the erbium-doped fiber and Er^{3+} ion is excited to level of E3. After a while, the excited ions starts to decay to the E2 through nonradioactive emission. Finally, the excited ions will falls to ground level through spontaneous emission and exhibit photon in 1520-1570nm wavelength region. The higher the pump power is pumped, the stronger the spontaneous emission amplified through entire fiber.

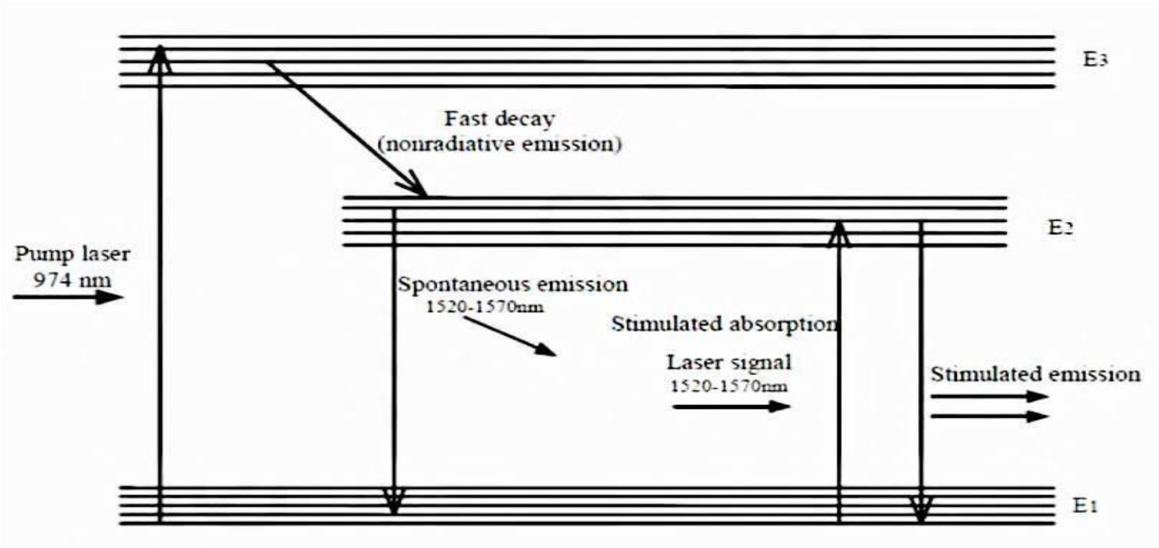

(Figure 1.3): **Diagram of energy levels in Erbium-doped fiber.**

5. Fiber Laser resonator

The behavior of resonators utilized in fiber lasers is comparable to that of conventional laser resonators. The essential differences between them are the geometry of the gain medium and the intra-cavity optical components. The fiber laser resonator optical components have specific characteristics, generally associated with the fiber coupling and tolerance for optical damages. The fiber laser gain medium's turn as an optical fiber waveguide with a considerably lengthier length than in conventional lasers. Besides, it has a so small optical medium diameter. The following section reviews the two most important types of laser resonators, which represent a significant part of practical fiber lasers.

1. Linear resonator

The optical linear resonator of fiber laser comprises mainly from two reflectors either ordinary dielectric mirrors which can be placed to the perpendicularly cleaved fiber ends or fiber Bragg gratings made either directly in the doped fiber, or in an undoped fiber which is spliced to the active fiber set in the optical cavity at opposite ends. Ion-rare-earth doped fiber gain medium, and the remain intra-cavity optical components are controlled the spectral and temporal characteristics of the fiber laser (Figure 1.4).

Resonant frequencies of the linear resonator are given by the following expression

$$\nu = M \frac{c_0}{2nL}$$

(Eq. 1.2)

Where *n* is the refractive index of the medium along the laser cavity length *L*. The propagation of optical waves in a linear resonator is in opposite directions between the two reflectors. The standing-waves are formed. They produce the spatial hole-burning phenomenon; this impacts the spatial gain distribution of the laser, which in turn desired in a multi-mode laser oscillation. As a result, the light propagates twice through the gain medium during the cavity roundtrip leading to account a double of the laser gain (and loss). On the other hand, the drawback of this system with relatively long cavity length and large gain- bandwidth suffers from rapid mode hopping effect because of the spatial hole burning.

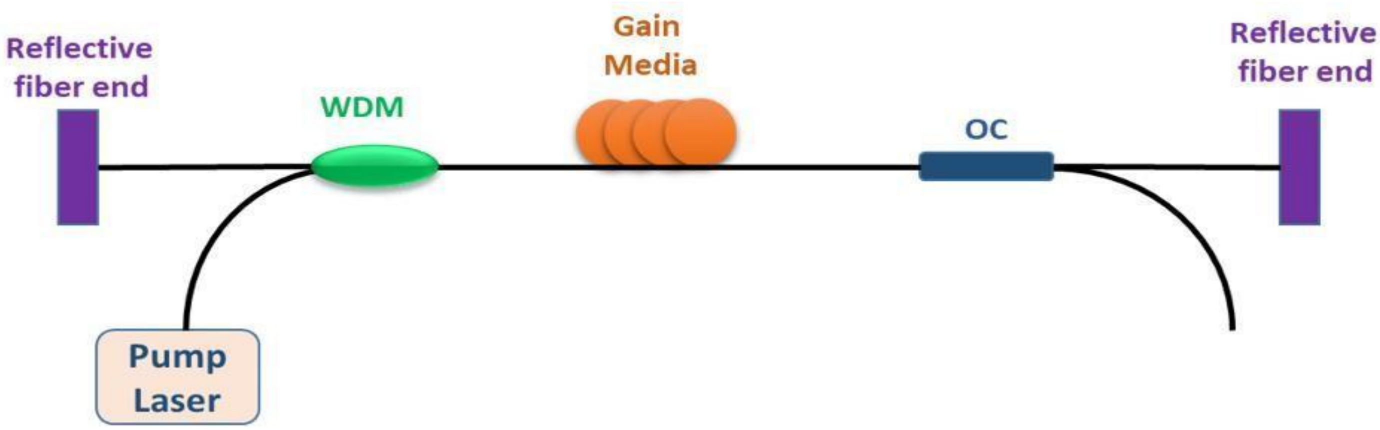

(Figure 1.4): **Linear resonator configuration.**

2. Ring resonator

The ring resonator is an essential one, realized as a resonator where the optical wave inside intra-cavity moves in a ring path. To attain a phase shift condition for the traveling light wave along the cavity roundtrip to be equivalent to 2π, the resonant frequency expression can be set as follows:

$$\nu = M \frac{c_0}{nL}$$

(Eq. 1.3)

However, different from linear resonators, the ring laser resonators as shown in Figure (1.5) employ unidirectional components like an optical isolator. It permits a unidirectional propagation of the optical waves in the fiber laser cavity; the concept of the cavity mode and cavity resonance frequency is no longer defined as the same wave as in the case of a standing wave resonator (linear resonator). In traveling wave (unidirectional) ring resonators, the gain and loss have to be counted once.

Less cavity roundtrip gain obviously reduces laser gain; while, the absence of a hole burning effect helps to achieve the single longitudinal mode of laser operation. Therefore, ring laser cavities are widely used for very narrow, single-longitudinal mode operation.

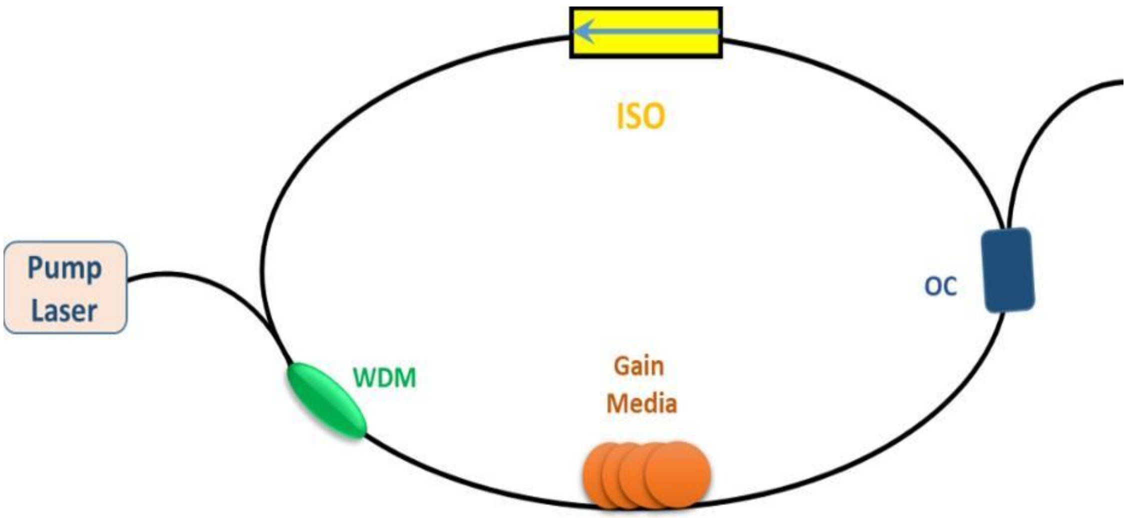

***(Figure 1.5)*: Ring resonator configuration.**

6. Q-switching

In 1961, the Q-switched operation starts with Hellwarth, who has come out with an idea which a short pulses can be produce if optical resonator loss quickly changes form high to low value [9]. After a year, proved their ideas with successful experimental demonstrations utilizing electrically switched Kerr cell shutter in ruby laser. Q-switched operation happens when the laser output of the cavity system is switched by controlling the resonator loss and thus, enables the generation of short pulses typically from nanosecond to picosecond.

Q-switch start to inhibit the feedback of light in gain medium when the gain medium is pumped continuously and will produces low Q in the optical resonator. This process generates the population inversion but since there is no feedback in the laser cavity, no laser is produced in this process. At the same time, stimulated emission continue to occur due to the gain medium being continuously pumped. After a certain time, the gain medium is saturated when the energy stored reaching their maximum value.

Suddenly, the Q-switch device switch rapidly from low to high Q which allows the feedback in the gain medium and starts to amplify the stimulated emission. Due to large energy stored in gain medium, the light intensity will build up very quickly and causes the gain depletion. As a result, a giant pulse produce from short pulse of light output which has high peak intensity. This process is called as Q-switching operation.

The cavity Q-factor formula is as follow:

$$\mathbf{Q} = \frac{\mathbf{2\pi f_o \varepsilon}}{\mathbf{P}}$$

(Eq. 1.4)

Where ***fo*** is resonant frequency, E is energy stored in cavity P = dE/dt is power dissipated.

Q-switched laser hold high potential and is widely used in applications which need a long duration of pulses such as environmental sensing and material processing are where Q-switched lasers are being utilized. Q-switching operations are divided into two types; ***active and passive.***

1. *Active Q-switching*

Active Q-switching require an external modulators such as mechanical, electro-optical or acousto-optics [10]. This method offers more complexity due to high losses in cavity system from the external modulators itself. Because of this drawbacks, researcher begin to find new alternative which leads to discovery of the passive Q- switching operation that give compact geometry and more simpler setup [11].

2. *Passive Q-switching*

For passive Q-switching operation, the SA is employed into laser cavity system by replacing the external modulator. The cavity laser system consists of gain medium and a nonlinear absorbing medium. When the gain medium is pumped, the energy is developed in the gain medium and thus emit the photons.

The laser may build when the gain medium become saturates before the absorber but the laser cannot emit intense pulse, but if the photons flux develops up to the level that saturates the absorber first, the laser resonator will form a quick reduction occurs in intracavity loss cause the laser Q-switched will produce short and intense pulse [12] .From the Semiconductor Saturable Absorber Mirror (SESAM) model by Spühler and his group [13] , they presented important parameters in passive Q- switched which are, repetition rate, pulse energy and pulse duration.

Figure 1.6 shows the pulse cycle which involves four different phase which g(t), q_o , q(t), Ag, g and

1 are round-trip intensity gain coefficient, unbleached value of saturable absorber per round-trip (bleached value of the saturable absorber, q=0),loss coefficient of a saturable absorber, gain coefficient between the beginning and the end of the pulse (gain reduction; $Ag=g_i-g_f$), saturated intensity gain coefficient per resonator round-trip and total I non-saturable loss coefficient per resonator round-trip.

At phase 1, absorber is initially at an unbleached state. When the gained is pumped until unsaturated value of losses, a pulse can be produce, the equation as following:

$$g_i=1+q_o \qquad \textbf{(Eq. 1.5)}$$

Where q_o is unbleached value of saturable absorber per round-trip and Ag is gain coefficient between the beginning and the end of the pulse (gain reduction; $Ag=g_i-g_f$). The intracavity power, P start to rise slowly from spontaneous emission noise till enough intensity to cause the bleaching of saturable absorber. Phase 2 begins when the SESAM is fully bleached (q=0) and when added this condition into Eq. 1.5, the new net gain which made the power grow rapidly until gain starts to deplete, shown in Eq 1.6.

$$g_i - 1 - q = q_o$$

(Eq. 1.6)

The maximum pulse achieved when the net gain is zero. Further depletion occurs in phase 3 and the gain become negative which made the intracavity start to decays. However, in this phase, the pulse still coupled out powerful energy. At phase 4, when the pulse of the absorber recover, the gain needs to be pumped to the threshold level again before the next pulse can start [14].

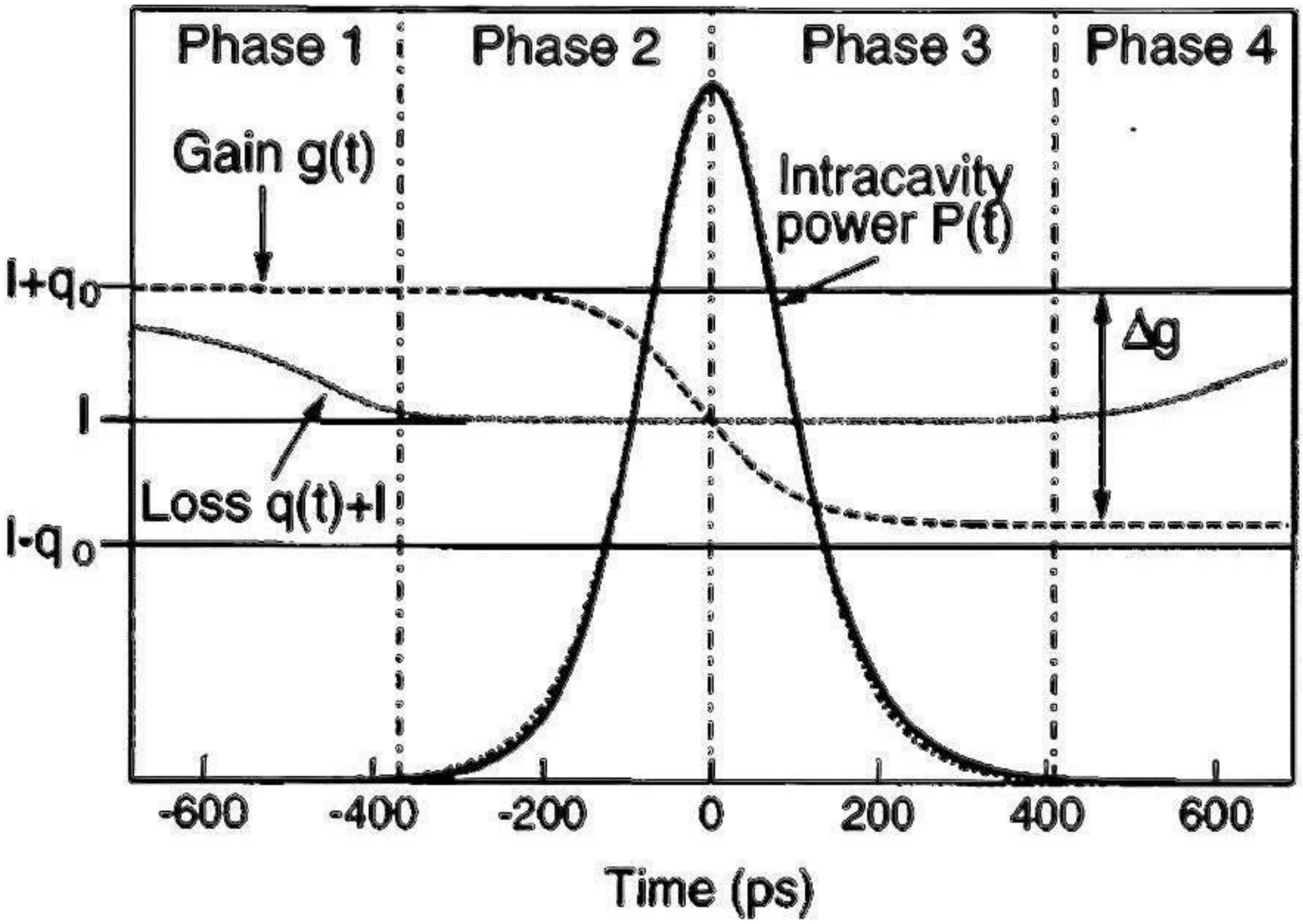

(Figure 1.6) The power, loss, and gain on time scale of the pulse width. After the gain surpass the loss, the power starts to develop. The peak of the Q-switched pulses is reached when the gain equals to the total losses.

7. Principle Of Saturable Absorber

The SA is a device which changes their absorbance in accordance to the power of the incident light. SA operation can be related to the principle of nonlinear saturable absorption, the transmission is larger at low optical intensities at high optical intensity.

Figure 1.7 shows the saturable absorption process in a two-level system [15]. When high optical intensity pass through the SA, $hv \geq E_g$ (band gap energy of the SA), the saturable absorption will occurs and suddenly induced electron-hole pair as constructed in Figure 1.7 (a). Meanwhile, excess photon energy, ($hv > E_g$) will produce electron kinetic energy and release as heat. High optical intensity will result a bigger different in the absorption rates of the SA. This can be relate to Pauli Exclusion Principle, when excited state is fully occupied, the absorption net will reduce and make the material saturated. Afterwards, light cannot absorbed and leave the SA transparent for light transmission, as presented in Figure 1.7 (b). The excited-state absorption and electron-hole recombination will happen when the subsequent light enter the SA [16].

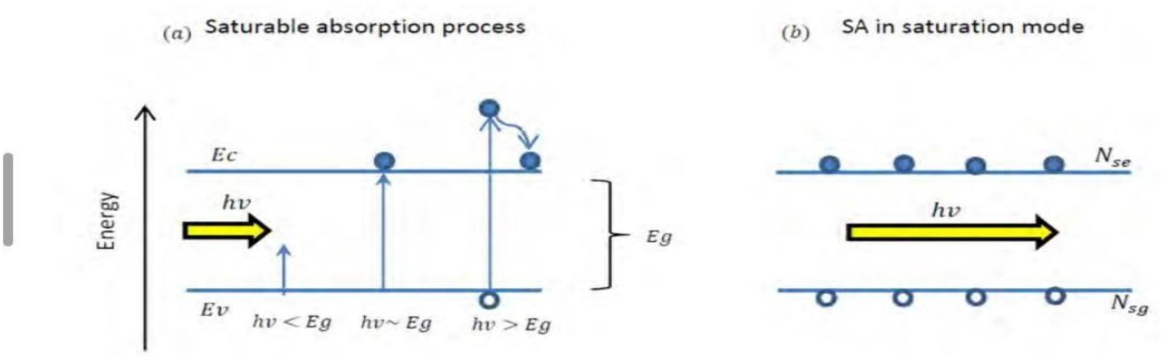

(Figure 1.7) **Formation of electron-hole pair in the saturable absorber of two level system with (a) saturable absorption process and (b) saturated SA.**

Generally, there have many methods to generate passive Q-switched including Semiconductor Saturable Absorber Mirror (SESAM), transition metal-doped bulk crystal, graphene, carbon nanotube (CNT), transition metal di-chalcogenides (TMDs), topological insulator (TI) and black phosphorus (BP). However, SESAMs drawbacks from high fabrication cost, fragility, limited operation bandwidth and needs extra optical component including lens and mirrors which added more complexity and high loss in cavity design [17]. Doped bulk crystals as SA also requires extra component such as mirror and lens to align the fiber output into the crystal [18]. The shortcomings of these two early approach has triggered researcher to find new SA which more compact and economical system.

Chapter Two Saturable Absorber

1. Introduction

In this chapter, we will explore zirconium dioxide-8ytria nanomaterial (ZrO_2-8Y) as saturable absorber (SA) in formed of thin film, then characterize its structure and optical properties to produce passive Q- switched laser. The used of SA with combination of EDF to generate passive Q-switched fiber laser is high potential in many applications such as telecommunication, spectroscopy, range finding and material processing.

2. Zirconium Dioxide-8Ytria nanomaterial

Zirconium Dioxide is a material of great technological importance, having good natural color, high strength, transformation toughness, high chemical stability, excellent corrosion resisting material, and chemical and microbial resistance. ZrO2 is a wide band gap p-type semiconductor that exhibits abundant oxygen vacancies on its surface. The high ion exchange capacity and redox activities make it useful in catalysis. ZrO2 is also an important dielectric material for potential application as an insulator in transistors in future nanoelectric devices. advanced metal oxide semiconductor (MOS) devices and in optical applications. Existence of Cubic ZrO2 until room temperature, which is named FSZ (fully stabilized zirconia), can be observed with concentration of 8% Yttria [19].

Stabilized zirconia in particular with Yttria called YSZ is widely used for a variety of applications such as thermal barrier material, and with additional optical characteristics such as transparency/ translucency, they are used as windows for anvil cells, infrared windows, laser host materials, armor applications, optical lenses, tooth-like esthetics, thermal insulating transparent windows, scratch- resistant electronics, bar scanners and high pressure sodium, and mercury halide lamps.

3. Preparation Method

The process of preparing a saturable absorbent material using three parts:-

- In the first part, a solution was prepared by dissolving 1g of PVA with 100ml of deionized (DI) water at a temperature of 75-90°C for an hour using a magnetic stirrer.
- In the second part, 5 ml of PVA solution was mixed with zirconium dioxide-8ytria (ZrO_2-8Y) at room temperature for an hour using a magnetic stirrer.
- Finally, the resulting mixture was carefully poured into a glass petri dish. The plate was left to dry naturally at room temperature over seven days until a layer of ZrO_2-8Y/PVA was formed.

The entire manufacturing process is carried out in a clean environment.

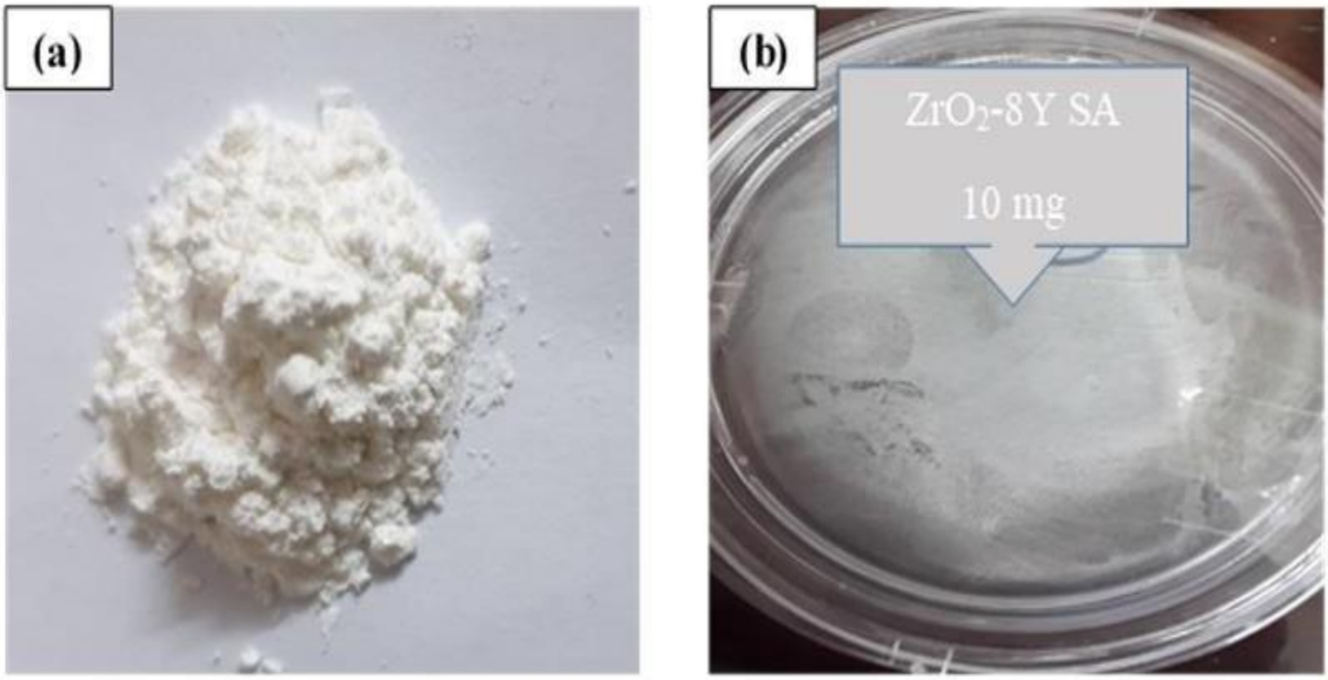

(Figure 2.1): **ZrO_2-8Y image of (a) nanopowder, (b) SA.**

4. *Characterization*

1. X-ray pattern

Figure (2.2) shows the X-ray pattern (XRD) of ZrO_2-8Y powder. This indicates peaks with 2θ values which are 30.01° (101), 34.74° (002), 50.11° (112), 59.60 (211^0), and 61.69 (202^0) without observing any impurity. The peaks indicate that the material has an excellent crystalline structure.

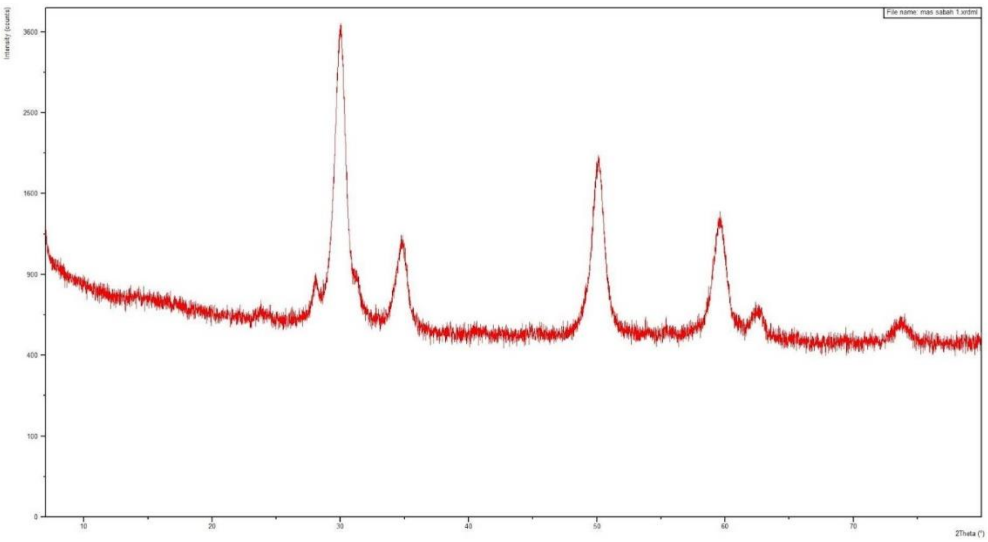

(Figure 2.2)**: XRD pattern of ZrO_2-8Y nano-powder**

2. Scanning Electron Microscope

The scanning electron microscope (SEM) image of ZrO_2-8Y nano-powder was taken as depicted in Figure (2.3). It is clearly show that the nano-crystalline morphology of the ZrO_2-8Y NPs is a homogenously and equally grain size with a spherical shape.

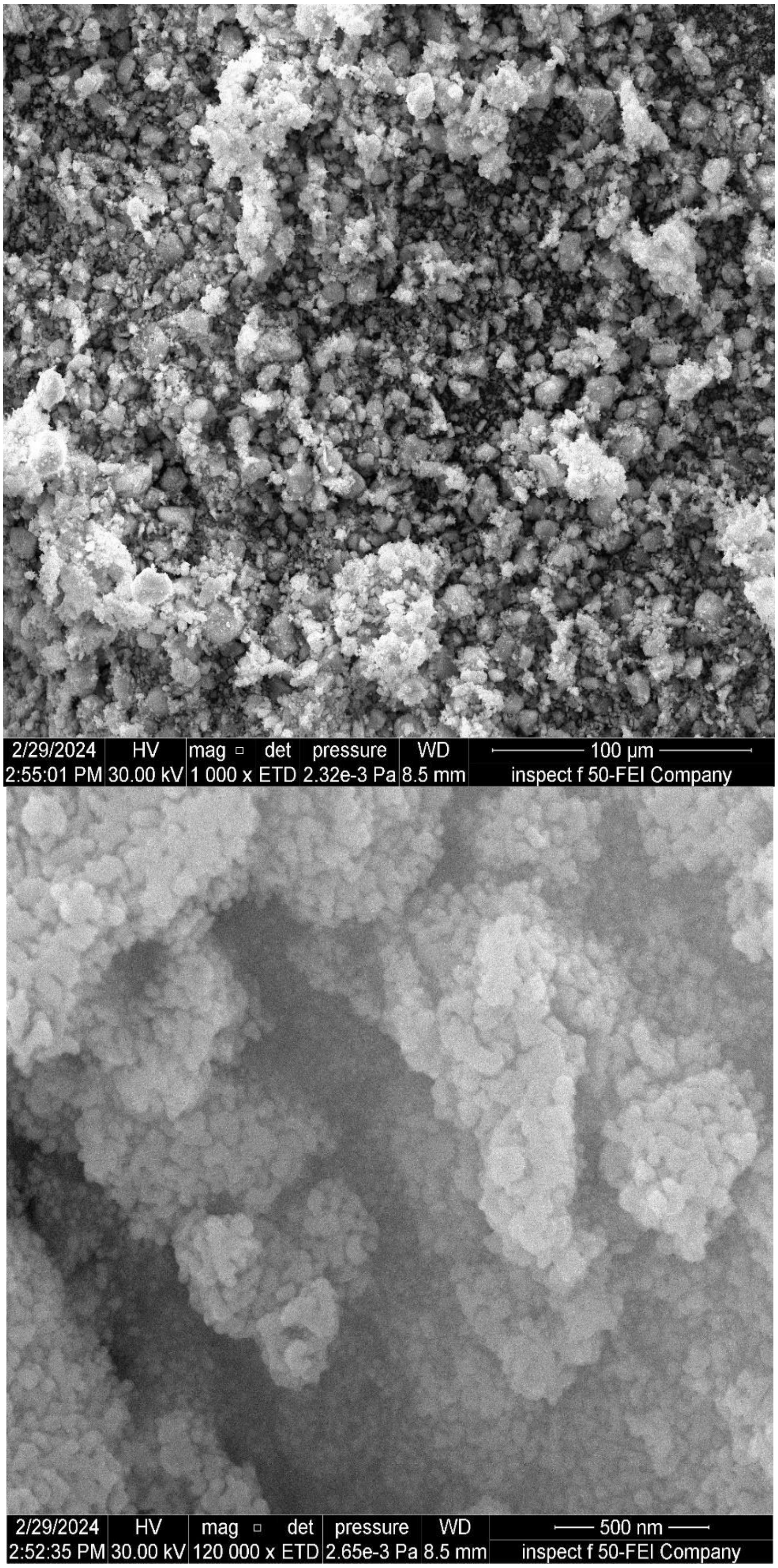

(Figure 2.3): (a) and (b) SEM of ZrO_2-8Y nano-powder images.

3. Optical Absorption

The optical properties of the ZrO_2-8Y/PVA thin film were studied based on its linear absorption spectra an optical spectrum analyzer (OSA) was used to analyze a broad range of low-intensity spectra, ranging from 1520 nm to 1570 nm, produced by a broadband light source to determine the linear absorption of the ZrO_2-8Y/PVA- SA. The results revealed that the thin film SA had a linear absorption of approximately 12 dBm at 1561 nm, as shown in Figure (2.4).

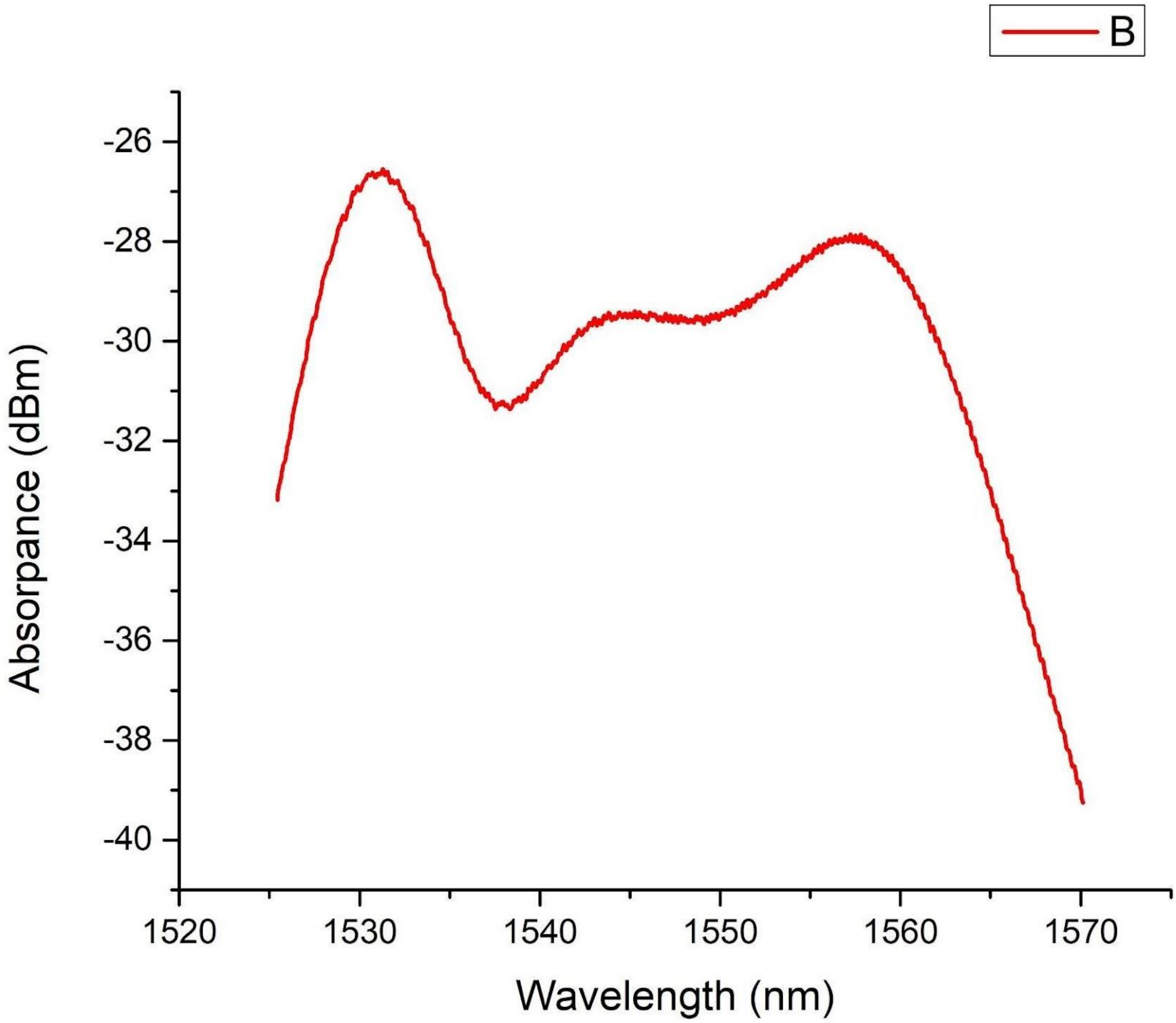

***(Figure 2.*4): Optical absorption of ZrO_2-8Y thin film.**

Chapter Three Result and Discussion

1. Introduction

Recently, there has been significant interest in Q-switched fiber lasers that operate in a microsecond pulse duration. They have a simple setup, are compact and flexible, and produce high-quality beams. These characteristics make them suitable for various applications, including material processing and medical treatments. There are two techniques for implementing Q-switched lasers, active and passive. Generally, the passive technique is favoured over the active technique as it offers multiple advantages. These include the ability to withstand harsh environments, ease of preparation, a smaller physical size, and the lack of a need for complex electronic circuits. Furthermore, the passive approach is more cost- effective.

In this chapter, the ZrO_2-8Y/PVA SA is applied in the fiber laser setting to generate Q-switching pulses.

2. *fiber laser setup*

The passively Q-switched EDFL configuration is depicted in Figure (3.1). The cavity included a 980/1550 nm wavelength division multiplexer (WDM), a gain medium of 1 m EDF having a numerical aperture range of 0.13, mode field diameter of 9.5 µm at 1550 nm, and a peak core absorption of 80 dB/m at 1530 nm. An isolator (ISO) to guarantee the unidirectional propagation of the laser and a 90/10 output coupler (O.C.) were placed in the cavity, where 90% of the light is fed back into the cavity, and the remaining 10% is the laser output. The SAs that were manufactured earlier was placed between two fiber ferrules with an FC/UPC connector using an index-matching gel. The EDF is pumped by a 976 nm laser diode (BL976-SAG300) by Temperature Controller with Mount.

The optical spectrum analyzer (OSA) (Fiber Mini optical spectrum analyzer,1525-1572 nm is utilized to examine the EDFL spectra with and without the SA, while the output pulse is analyzed with a 2 GHz/s digital storage oscilloscope (OSC) through a photodetector is (Thorlabs) DET10C, 700-1800 nm. Additionally, an optical power meter is used to measure the output power. The full length of the cavity is about 3 m.

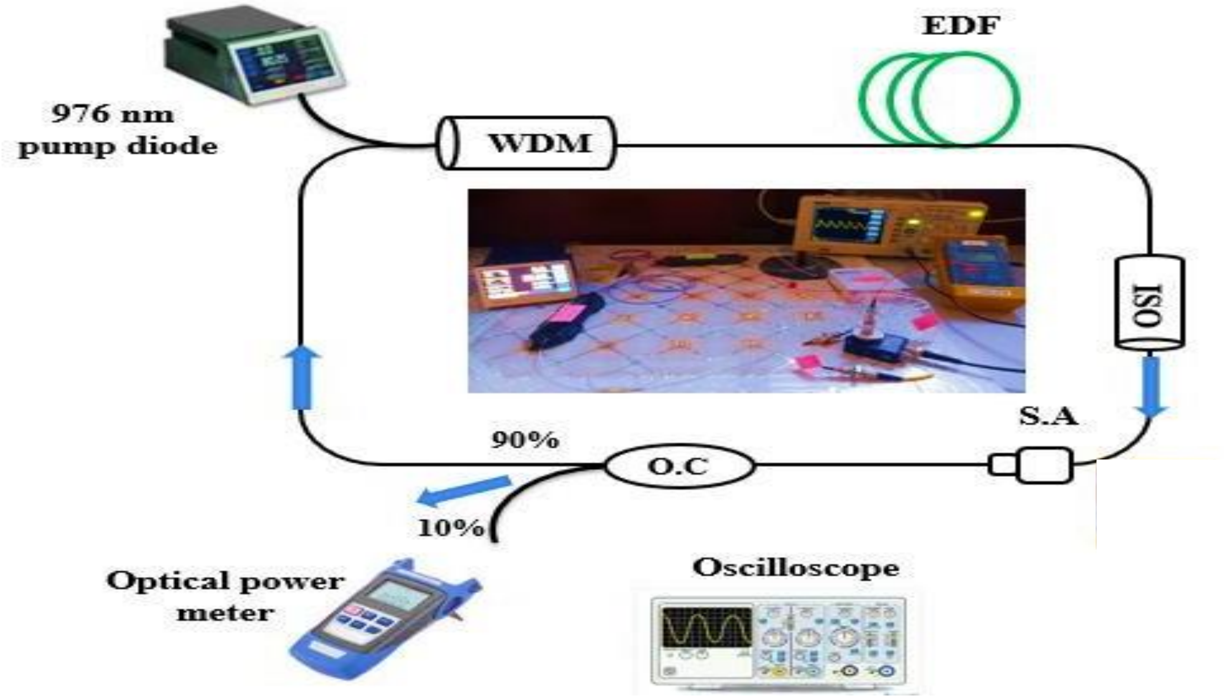

Figure (3.1): The configuration of the ring laser cavity.

3. *Q-switching Result and Discussion*

The details and the characteristics of the passive Q-switched fiber laser output are illustrated. Self-starting and stable Q-switching pulses has been recorded at 200 mW threshold pump power, and it sustains to be stable until reached to maximum available input pump power of 280 mW. The ZrO_2- 8Y/PVA SA is conserved stably without any thermal damage during the experiment. Figure (3.2 a) depicts the oscilloscope trace of the Q-switching train pulses obtained at maximum input pump power of 275 mW.

The train of pulses display a stable Q-switching operation devoid of any fluctuations. The shortest single pulse envelop profile is shown in Figure (3.2 b), which points out a FWHM of 10.5 µs. The pulse appears to be symmetrical, and has a uniform shape.

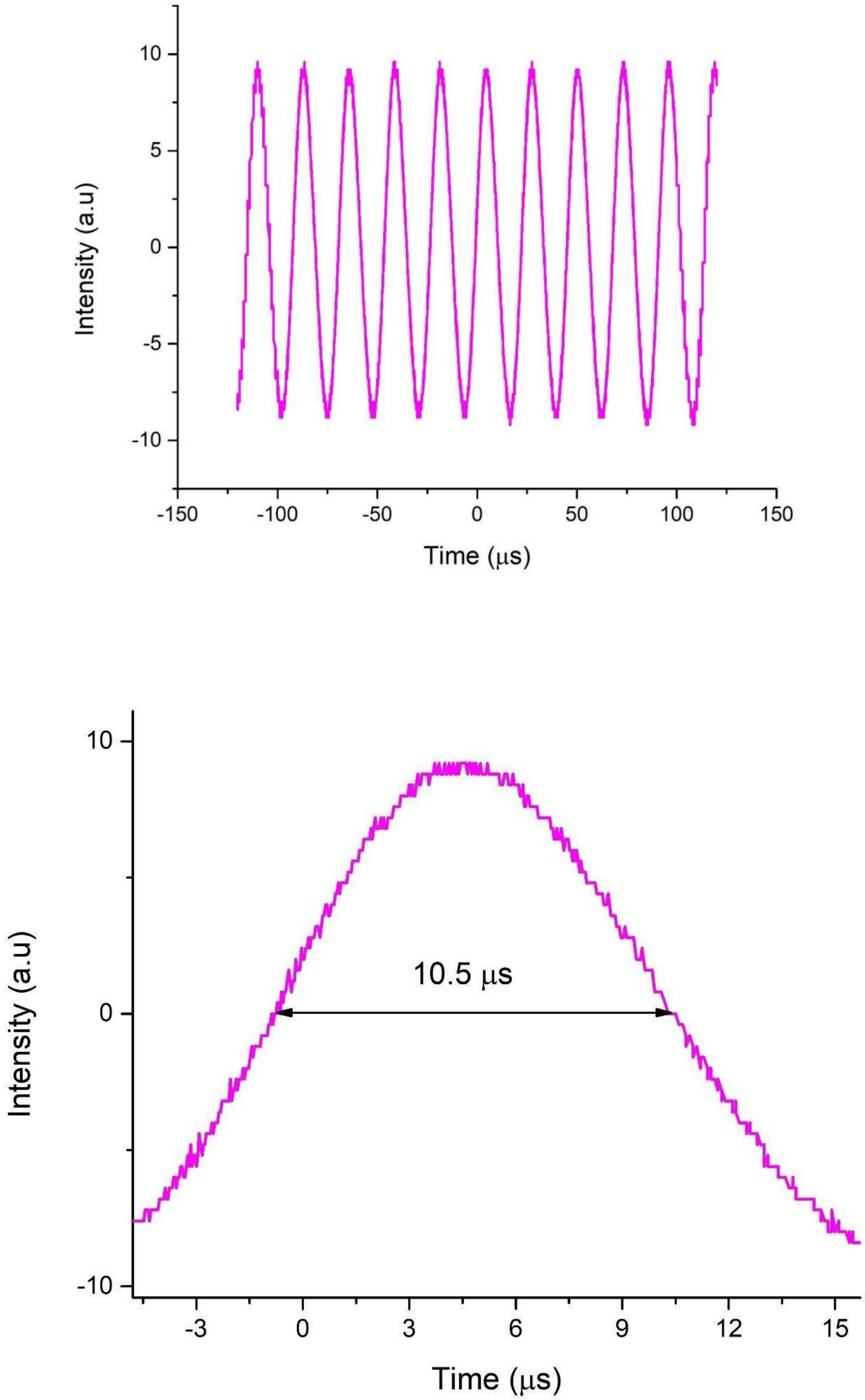

(Figure 3.2): **Oscilloscope trace for EDFL (a) Pulse train under the pump power of 280 mW with a repetition rate of 52.5 kHz (b) Single pulse trace under a pump power of 280 mW.**

Figure (3.3) presents the variation of the pulse width and pulse repetition rate of the Q- switching fiber laser related to the input pump power. When the pump power raises from 200 to 280 mW, the pulse width reduces from 14.3 to 10.5 μs, while laser repetition rate increases from 43.7 to 52.5 kHz. This behavior can be clarified that the higher input pump power accumulates more electrons in the saturable absorber upper level. Therefore, the pulse width becomes shorter via reducing the pulse rise time and the falling.

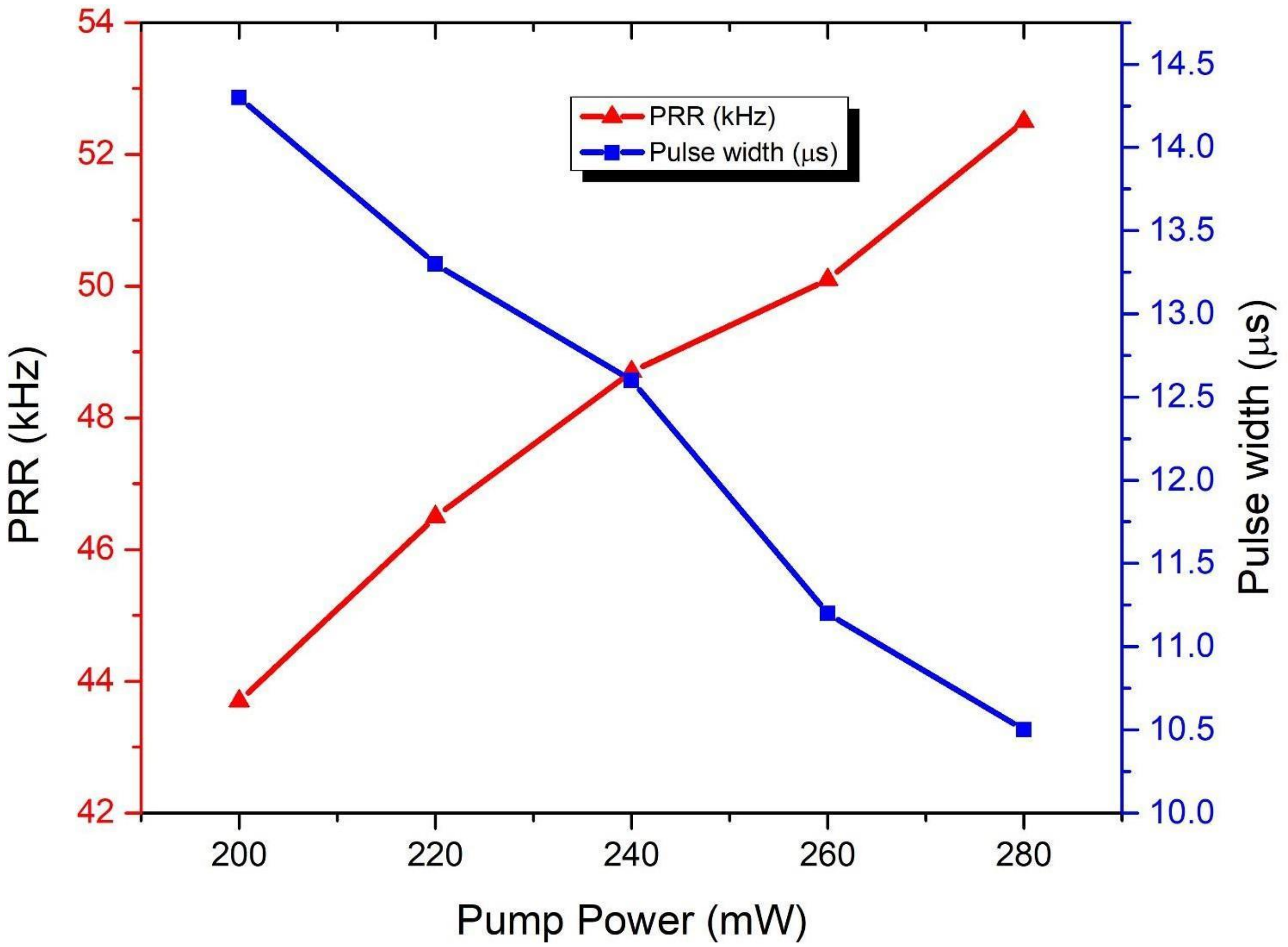

(Figure 3.3): **Pulse repetition rate and pulse width vs. pump power.**

Moreover, the measured average output power which increased linearly from 95 - 151.7 μs as the pump power varied from 200 mW to 280 mW, as depicted in Figure (3.4). Generally, the rise in the input pump power amplifies the gain leading to an increase in the average output power. As a result, the increasing in output power will reduce the pulse width, and increase the pulse energy in the Q-switching process.

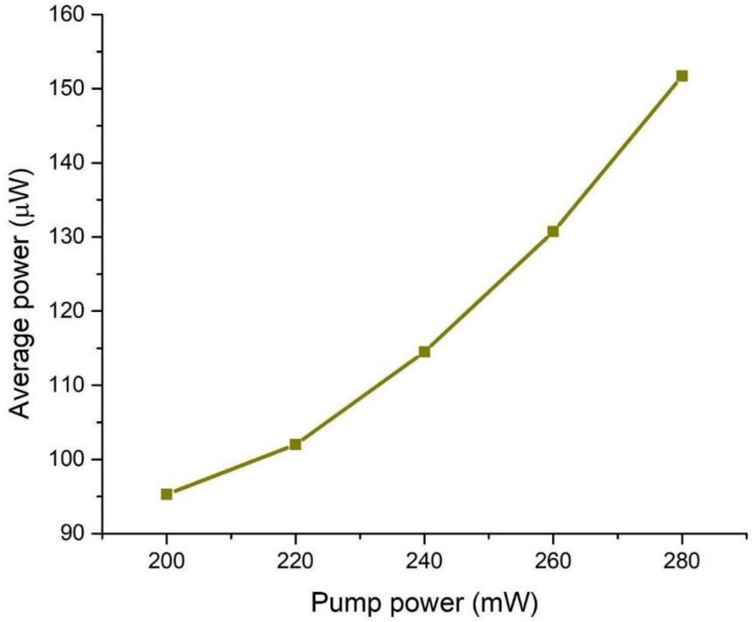

(Figure 3.4): **Output power vs. pump power.**

Figure (3.5) depicts the laser output wavelengths for Q-switched operations (with SA) at a maximum pump power of 280 mW. The optical spectrum of the EDFL with a central wavelength is 1561 nm.

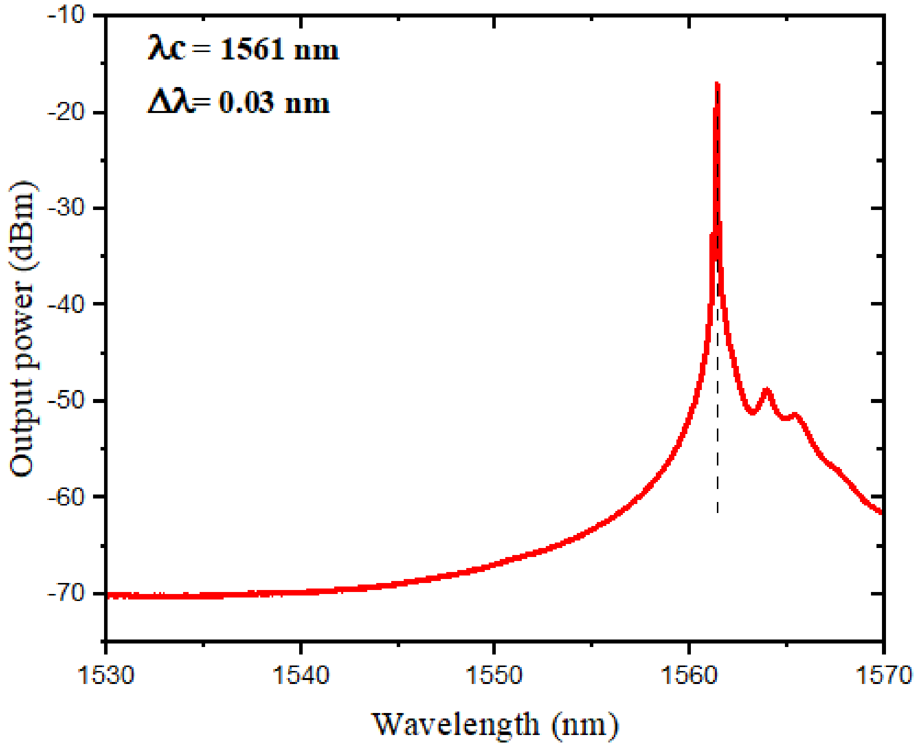

(Figure 3.5): **Q-switched EDFL optical spectrum Measured at a pump power of 280 mW.**

Chapter Four Conclusion and Future Work

1. Conclusion

By employing a film-based SA as a Q-switcher, a passive Q-switched EDFL was created. With repetition rates rising from 43.7kHz to 52.5 kHz and pulse widths falling from 14.3 µs to

10.5 µs, the Q-switching operation was accomplished effectively. These findings confirm that ZrO_2-8Y has optical characteristics that are beneficial for SA applications in reasonably priced Q-switched EDFLs.

2. Future Work

An analysis of Q-switching operation for the use of ZrO_2-8Y nanomaterials in ytterbium, thulium, and holmium-doped fibers.

References

1. Morkel, P. R., K P. Jedrzejewski, E. R. Taylor, and D. N. Payne. "Short-Pulse, HighPower Q-Switched Fiber Laser." IEEE Photonics Technology Letters, vol. 4, no. 6, June 1992, pp. 545-47. Accessed 2016.
2. Adachi, Shoji, and Yahei Koyamada. "Analysis and Design of Q-Switched ErbiumDoped Fiber Lasers and Their Application to OTDR." Journal of Lightwave Technology, vol. 20, no. 8, Aug. 2002, pp. 1506-10. Accessed 2016.
3. Eichhorn, Marc. "Development of a high-pulse-energy Q-switched Tm-doped doubleclad fluoride fiber laser and its application to the pumping of mid-IR lasers." OPTICS LETTERS, vol. 32, no. 9, May 2007, pp. 1056-58. Accessed 2016.
4. Kurkov, A. S. "Q-switched all-fiber lasers with saturable absorbers." Laser Physics Letters, vol. 8, no. 5, Mar. 2011, pp. 335-41. Accessed 2016.
5. Set, Sze Y., Hiroshi Yaguchi, Yuichi Tanaka, and Mark Jablonski. "Ultrafast Fiber Pulsed Lasers Incorporating Carbon Nanotubes." IEEE Journal of Selected Topics in Quantum Electronics, vol. 10, no. 1, Feb. 2004, pp. 137-45. Accessed 2016.
6. Svelto, O., & Hanna, D. C. (1998). Principles of lasers
7. Kao, K., & Hockham, G. A. (1966). Dielectric-fibre surface waveguides for optical frequencies. Paper presented at the Proceedings of the Institution of Electrical Engineerings.
8. Desurvire, E., & Simpson, J. R. (1989). Amplification of spontaneous emission in erbium-doped single-mode fibers. JOURNAL OF LIGHTWAVE TECHNOLOGY, 7(5), 835-845. doi:10.1109/50.19124.
9. Hellwarth, R. (1961). Advances in quantum electronics: Columbia Press, New York.
10. Koechner, W. (2006). Q-Switching Solid-State Laser Engineering (pp. 488-533). New York, NY: Springer New York.
11. Svelto, O., & Hanna, D. C. (1998). Principles of lasers.
12. Welford, D. (2003). Passively Q-switched lasers. IEEE circuits and devices magazine.
13. Spühler, G., Paschotta, R., Fluck, R., Braun, B., Moser, M., Zhang, G., ... Keller, U. (1999). Experimentally confirmed design guidelines for passively Q-switched microchip lasers using semiconductor saturable absorbers. JOSA B, 16(3), 376- 388.
14. Spühler, G., Paschotta, R., Fluck, R., Braun, B., Moser, M., Zhang, G.,... Keller, U. (1999). Experimentally confirmed design guidelines for passively Q-switched microchip lasers using semiconductor saturable absorbers. JOSA B, 16(3), 376- 388.
15. Zulkifli, A. Z. (2015). Fabrication and characterisation of graphene oxide saturable absorber for Q-Switched fiber laser generation/Ahmad Zarif bin Zulkifli. University of Malaya.
16. Kashiwagi, K., & Yamashita, S. (2010). Optical Deposition of Carbon Nanotubes for Fiber-based Device Fabrication. In B. Pal (Ed.), Frontiers in Guided Wave Optics and Optoelectronics (pp. Ch. 19). Rijeka: InTech.
17. Okhotnikov, O., Grudinin, A., & Pessa, M. (2004). Ultra-fast fibre laser systems based on SESAM technology: new horizons and applications. New journal of physics, 6(1), 177.

18. Laroche, M., Chardon, A., Nilsson, J., Shepherd, D., Clarkson, W., Girard, S., & Moncorgé, R. (2002). Compact diode-pumped passively Q-switched tunable Er- I Yb double-clad fiber laser. Optics letters, 27(22), 1980-1982.

19. J. Winczewski, S. Zeiler, S. Gabel, D. Maestre, B. Merle, J. Gardeniers, et al., "Additive manufacturing of 3D yttria- stabilized zirconia microarchitectures," Materials & Design, vol. 238, p. 112701, 2024.